Four-pion production in τ decays and e^+e^- annihilation: An update

Henryk Czyż
Institute of Physics, University of Silesia, PL-40007 Katowice, Poland

Johann H. Kühn
Institut für Theoretische Teilchenphysik, Universität Karlsruhe, D-76128 Karlsruhe, Germany

Agnieszka Wapienik
Institute of Physics, University of Silesia, PL-40007 Katowice, Poland
(Received 3 April 2008; published 6 June 2008)

An improved description of four-pion production in electron-positron annihilation and in τ-lepton decays is presented. The model amplitude is fitted to recent data from *BABAR* which cover a wide energy range and which were obtained exploiting the radiative return. Predicting τ-decay distributions from e^+e^- data and comparing these predictions with ALEPH and CLEO results, the validity of isospin symmetry is confirmed within the present experimental errors. A good description of two- and three-pion subdistributions is obtained. Special emphasis is put on the predictions for $\omega\pi(\to \pi^+\pi^-\pi^0)$ in e^+e^- annihilation and in τ decay. The model amplitude is implemented in the Monte Carlo generator PHOKHARA.

DOI: 10.1103/PhysRevD.77.114005 PACS numbers: 13.66.Bc, 12.40.Vv, 13.35.Dx

I. INTRODUCTION

The production of four pions in τ decays and e^+e^- annihilation has received considerable attention, both from the theoretical [1–9] and the experimental side [10–17]. Relating the cross sections and rates for the four charge combinations ($\pi^+\pi^-2\pi^0$, $2\pi^+2\pi^-$, $2\pi^-\pi^+\pi^0$, and $\pi^-3\pi^0$) gives important hints on the validity of isospin symmetry and the size of the isospin breaking terms. The dependence of the rates and the cross sections on $\sqrt{Q^2}$, the invariant mass of the four-pion system, and the investigation of differential distributions, e.g. of the two- and/or three-pion masses, gives information on the resonance structure of the amplitude. In the low Q^2 region, predictions based on the chiral Lagrangian can be tested which, however, must be complemented by resonance physics in order to properly describe the rates in the dominant region between 1 and 3 GeV. The e^+e^- cross section is, furthermore, important to evaluate the hadronic vacuum polarization which in turn is essential for the precise prediction of the muon anomalous magnetic moment and the running of the electromagnetic coupling [18,19].

From the experimental side precise τ data have been obtained by ALEPH [15] and by CLEO [11] collaborations, which, however, are naturally restricted to $\sqrt{Q^2}$ below 1.77 GeV. The e^+e^- cross section has been measured by CMD2 [10,12,14] and SND [13] (older data are far less accurate and will be not used in this paper) and, more recently, by *BABAR* [16,17] through the method of radiative return which covers energies up to 4.5 GeV. This method, which was proposed in [5,20,21], allows to use the large luminosity at B-factories for a measurement of the e^+e^- cross section in the region of interest.

From the theory side the first evaluation based on chiral perturbation theory has been performed by Fischer, Wagner, and Wess [1] and applied to τ decays. Subsequently this ansatz was extended [3] to include ρ, a_1, and f_0 resonances, which are clearly visible in subdistributions. In addition the $\omega\pi$ mode was introduced, again predicted from the chiral anomaly [2,6]. Later this ansatz, slightly modified, was implemented in the generator EVA [21] to simulate 4π production in the radiative return [5]. As stated above, the low Q^2 region should be best suited for a description based on chiral Lagrangians. Combining one-loop chiral corrections at low Q^2 with resonance enhancements at intermediate energies, precise predictions have been obtained in [6] which will be discussed below.

In view of these recent theoretical and experimental developments, together with need for an optimal implementation of the 4π mode into the Monte Carlo event generator PHOKHARA [22–29], an improved ansatz for the corresponding hadronic amplitude has been developed. The ansatz is largely based on [3,5] and [28] (concerning the ω part) with model parameters fitted to the recent *BABAR* results. In order to accommodate the $\rho^+\rho^-$ signal observed in [17] we include a contribution, which is modeled to mimic a $SU(2)$ gauge theory with the ρ-meson (and its radial excitations) as gauge boson(s).

Our paper is organized as follows: To facilitate the subsequent discussion, in Sec. II the basic definitions are introduced and the (well-known) isospin relations between the amplitudes and the rates of the four channels are collected. The validity of these relations is investigated in Sec. III, using data from e^+e^- annihilation to predict the corresponding, experimentally measured distributions for τ decays. The ingredients for the ansatz for the matrix

element of the hadronic current are discussed in Sec. IV. The comparison of this ansatz with e^+e^- data and the fit of its parameters is presented in Sec. V together with the comparison between the model and data for a variety of distributions. The implications of the model for τ decays is discussed in Sec. VI, the implementation into the generator PHOKHARA and related technical tests in Sec. VII. A brief summary and our conclusions are given in Sec. VIII. A detailed description of our model with the complete list of parameters can be found in the Appendix.

II. GENERAL PROPERTIES OF THE FOUR-PION ELECTROMAGNETIC CURRENT

General properties of the four-pion electromagnetic current were investigated in [4], where it was shown that assuming isospin symmetry just one function J_μ describes all four matrix elements. We use the same letter J for the operator and its matrix element. For convenience we recall the definitions and notation introduced in [4,5].

Ignoring the issues of isospin breaking and radiative corrections, the electromagnetic current can be decomposed into an isospin singlet piece and a part transforming like the third component of an isospin triplet:

$$J^{em} = \frac{1}{\sqrt{2}} J^3 + \frac{1}{3\sqrt{2}} J^{I=0}, \tag{1}$$

whereas the charged current generating τ decays is given by

$$J^- = \frac{1}{\sqrt{2}}(J^1 - iJ^2). \tag{2}$$

Final states with an even number of pions are produced through the isospin one part only

$$\begin{aligned}
\langle \pi^+\pi^-\pi_1^0\pi_2^0|J_\mu^3|0\rangle &= J_\mu(p_1, p_2, p^+, p^-),\\
\langle \pi_1^+\pi_2^+\pi_1^-\pi_2^-|J_\mu^3|0\rangle &= J_\mu(p_2^+, p_2^-, p_1^+, p_1^-)\\
&\quad + J_\mu(p_1^+, p_2^-, p_2^+, p_1^-)\\
&\quad + J_\mu(p_2^+, p_1^-, p_1^+, p_2^-)\\
&\quad + J_\mu(p_1^+, p_1^-, p_2^+, p_2^-),\\
\langle \pi^-\pi_1^0\pi_2^0\pi_3^0|J_\mu^-|0\rangle &= J_\mu(p_2, p_3, p^-, p_1)\\
&\quad + J_\mu(p_1, p_3, p^-, p_2)\\
&\quad + J_\mu(p_1, p_2, p^-, p_3),\\
\langle \pi_1^-\pi_2^-\pi^+\pi^0|J_\mu^-|0\rangle &= J_\mu(p^+, p_2, p_1, p^0)\\
&\quad + J_\mu(p^+, p_1, p_2, p^0).
\end{aligned} \tag{3}$$

The function $J_\mu \equiv J_\mu(q_1, q_2, q_3, q_4)$ is symmetric (antisymmetric) with respect to the interchange of q_1 and q_2 (q_3 and q_4).

In [6] it was shown that also the matrix element $\langle \pi_1^-\pi_2^-\pi^+\pi^0|J_\mu^-|0\rangle$ can be used as an independent function, through which the other ones can be expressed. If one denotes

$$\langle \pi^-\pi_1^0\pi_2^0\pi_3^0|J_\mu^-|0\rangle = F_\mu(p_1, p_2, p^-, p_3), \tag{4}$$

one gets relation

$$\begin{aligned}
\langle \pi_1^+\pi_2^+\pi_1^-\pi_2^-|J_\mu^3|0\rangle &= F_\mu(p_2^+, p_2^-, p_1^+, p_1^-)\\
&\quad + F_\mu(p_2^+, p_1^+, p_2^-, p_1^-),
\end{aligned} \tag{5}$$

from which it is clear that the matrix element $\langle \pi_1^+\pi_2^+\pi_1^-\pi_2^-|J_\mu^3|0\rangle$ can be expressed by the matrix element $\langle \pi^-\pi_1^0\pi_2^0\pi_3^0|J_\mu^-|0\rangle$. The opposite is also true and we have proved it using the method developed in [6] to express $\langle \pi^+\pi^-\pi_1^0\pi_2^0|J_\mu^3|0\rangle$ by $\langle \pi_1^-\pi_2^-\pi^+\pi^0|J_\mu^-|0\rangle$. However, as in both cases the obtained inverse relations are far from being as elegant as the ones of Eq. (3) and (5); the result is not presented here.

The currents defined in Eq. (3) contain the complete information about the hadronic cross section through

$$\begin{aligned}
&\int J_\mu^{em}(J_\nu^{em})^* d\bar{\Phi}_n(Q; q_1, \ldots, q_n)\\
&\quad = \frac{1}{6\pi}(Q_\mu Q_\nu - g_{\mu\nu}Q^2)R(Q^2),
\end{aligned} \tag{6}$$

where $R(Q^2)$ is equal to $\sigma(e^+e^- \to \text{hadrons})(Q^2)/\sigma_{\text{point}}$, with $\sigma_{\text{point}} = 4\pi\alpha^2/(3Q^2)$, and $d\bar{\Phi}_n(Q; q_1, \ldots, q_n)$ denotes the n body phase space with all statistical factors included.

The amplitude describing the τ decay into an arbitrary number of hadrons plus a neutrino (excluding radiative corrections) is given by

$$\mathcal{M}_\tau = \frac{G_F}{\sqrt{2}} V_{ud}\bar{\nu}(p_\nu)\gamma^\alpha(1-\gamma_5)u(p_\tau)J_\alpha^-, \tag{7}$$

with

$$J_\alpha^- \equiv J_\alpha^-(q_1, \ldots, q_n) \equiv \langle h(q_1), \ldots, h(q_n)|J_\alpha^-(0)|0\rangle \tag{8}$$

and $J_\alpha^-(0) \equiv \bar{d}\gamma_\alpha u$ at the quark level, where we restrict our considerations to the Cabbibo allowed vector part of the hadronic current.

The differential τ decay rates are given by

$$\begin{aligned}
\frac{d\Gamma_{\tau\to\nu+\text{hadrons}}}{dQ^2} &= 2\Gamma_e \frac{|V_{ud}|^2 S_{\text{EW}}}{m_\tau^2}\left(1-\frac{Q^2}{m_\tau^2}\right)^2\\
&\quad \times \left(1+2\frac{Q^2}{m_\tau^2}\right)R^\tau(Q^2),
\end{aligned} \tag{9}$$

with

$$\begin{aligned}
\int J_\mu^- J_\nu^{-*} d\bar{\Phi}_n(Q; q_1, \ldots, q_n) &= \frac{1}{3\pi}(Q_\mu Q_\nu - g_{\mu\nu}Q^2)\\
&\quad \times R^\tau(Q^2)
\end{aligned} \tag{10}$$

and $\Gamma_e = G_F^2 m_\tau^5/(192\pi^3)$. Note the relative factor of 2 between the definitions in Eqs. (6) and (10). We have included here also the electroweak correction factor S_{EW}

(we use $S_{\rm EW} = 1.0198$ [7]) to account for standard electroweak corrections.

The function R^τ is related to the spectral function defined by CLEO [11] through $R^\tau(--+0) = 3\pi V^{3\pi\pi^0}$ and through $R^\tau = 3v_1$ to the vector spectral functions defined by ALEPH [15]. In this paper we will use normalization of the spectral functions chosen by ALEPH.

The four-pion spectral functions and the cross sections can be expressed as linear combinations of two integrals

$$A = -\frac{2\pi}{Q^2}\int J^\mu(q_1,q_2,q_3,q_4)J^*_\mu(q_1,q_2,q_3,q_4) \times d\Phi_4(Q;q_1,\ldots,q_4),$$
$$B = -\frac{4\pi}{Q^2}\int \mathrm{Re}(J^\mu(q_1,q_2,q_3,q_4) \times J^*_\mu(q_1,q_3,q_2,q_4))d\Phi_4(Q;q_1,\ldots,q_4). \quad (11)$$

The relations read

$$R(+-00) = \tfrac{1}{2}A; \qquad R^\tau(--+0) = A + \tfrac{1}{2}B;$$
$$R(++--) = A + B; \qquad R^\tau(-000)+ = \tfrac{1}{2}(A+B). \quad (12)$$

The additional contribution to $R(++--) = A + B + C$ of the form

$$C = -\frac{2\pi}{Q^2}\int \mathrm{Re}(J^\mu(q_1,q_2,q_3,q_4) \times J^*_\mu(q_3,q_4,q_1,q_2))d\Phi_4(Q;q_1,\ldots,q_4), \quad (13)$$

vanishes for any symmetric phase space configuration. Equations (12) correspond to the familiar relations between τ decay rates and e^+e^- annihilation cross sections:

$$R^\tau(-000) = \tfrac{1}{2}R(++--),$$
$$R^\tau(--+0) = \tfrac{1}{2}R(++--) + R(+-00). \quad (14)$$

III. ISOSPIN SYMMETRY—EXPERIMENTAL SITUATION

In this section we would like to address the question, if present experiments require inclusion of isospin violating effects in the model. Combining the results from *BABAR* [16] on $\sigma(e^+e^- \to 2\pi^+2\pi^-)$ with their preliminary results on $\sigma(e^+e^- \to 2\pi^0\pi^+\pi^-)$ [17] and using Eqs. (14), one obtains predictions for the τ spectral functions. These can be compared with ALEPH [15] and CLEO [11] data (compare also [17]). As shown in Fig. 1 and Fig. 2, τ and e^+e^- data are in good agreement within the errors, even if one observes systematical shifts. However, these shifts are well within the 5% systematic error of CLEO and the 6% ($2\pi^-\pi^+\pi^0$) and 10% ($\pi^-3\pi^0$) errors for ALEPH spectral functions (ALEPH does not give separately the systematic error) as well as the 5% to 12% systematic error for *BABAR* $\sigma(e^+e^- \to 2\pi^+2\pi^-)$. For the preliminary *BABAR* data

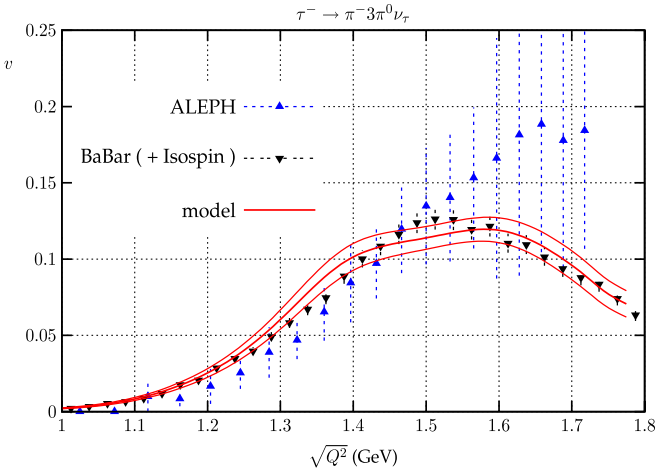

FIG. 1 (color online). The spectral function of the $\tau^- \to \nu 3\pi^0\pi^-$ decay mode. ALEPH data [15] versus predictions from *BABAR* data [16,17] and the model predictions.

[17] on $\sigma(e^+e^- \to 2\pi^0\pi^+\pi^-)$ a 10% systematic error is assumed. Truly isospin breaking effects are expected to occur at the percent level due to the $\pi^\pm - \pi^0$ mass difference alone [5].

From the cross section $\sigma(e^+e^- \to 2\pi^0\pi^+\pi^-)$ and the relative contributions of the $\omega\pi$ final state as given in [17] (since the errors were not specified there, we attribute 20% error to the spectrum) one can infer the ω contribution to $\sigma(e^+e^- \to 2\pi^0\pi^+\pi^-)$. Based on this result one can predict the omega part of the $\tau^- \to \nu 2\pi^-\pi^+\pi^0$ spectral function and compare it with the CLEO result. Satisfactory agreement is observed in Fig. 3.

From the comparisons of experimental data we conclude that no isospin symmetry violation is observed within the present accuracy. Thus the model we propose to describe the data is based on isospin symmetry. However, effects

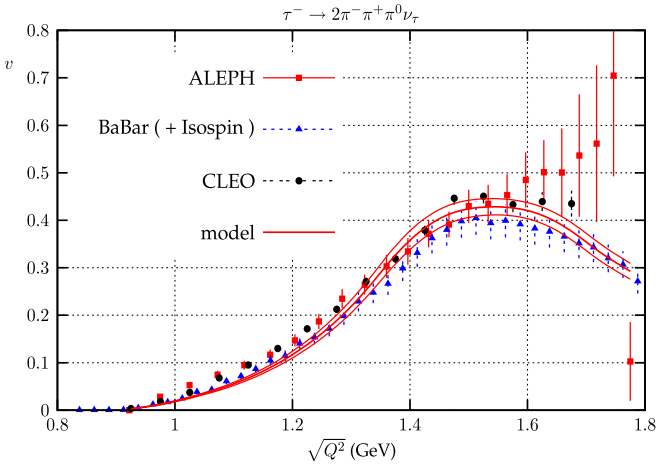

FIG. 2 (color online). The spectral function of the $\tau^- \to \nu 2\pi^-\pi^+\pi^0$ decay mode. ALEPH [15] and CLEO [11] data versus predictions from *BABAR* data [16,17] and the model predictions.

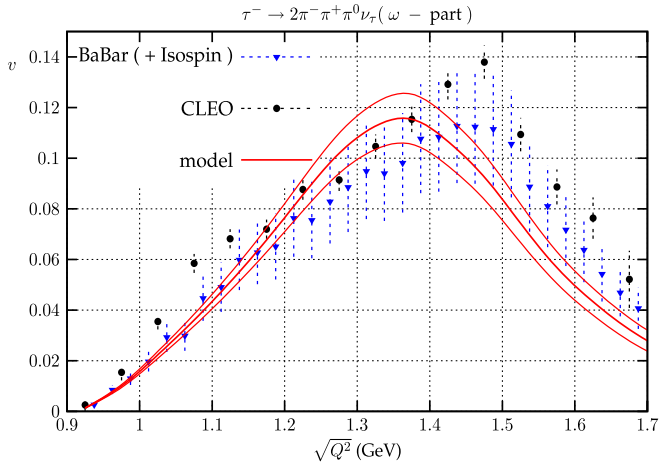

FIG. 3 (color online). The omega part of the spectral function of the $\tau^- \to \nu 2\pi^-\pi^+\pi^0$ decay mode. CLEO [11] data versus predictions based on preliminary *BABAR* data [17] and the model predictions.

from the pion mass difference in the phase space are included.

IV. THE MODEL OF THE FOUR-PION ELECTROMAGNETIC CURRENT

There are many motivations why the model adopted in [5] should be updated. First of all new and more accurate data are available. The CLEO data on tau decays [11], which were not used in [5], the tau spectral functions from ALEPH [15], and the measurement of the cross section of the reaction $e^+e^- \to 2\pi^+2\pi^-$ via the radiative return method by *BABAR* [16] provide us with the opportunity for a substantial improvement of the model implemented in the event generator PHOKHARA [22–29]. The omega part of the current, which in [3,5] was implemented without structure, is now known much better from phenomenological studies [28]. The new preliminary data from *BABAR* [17] on the reaction $e^+e^- \to 2\pi^0\pi^+\pi^-$ also show richer structure than implemented in [5]. All this was taken into account in constructing the model presented in this paper.

The amplitude used in [5] is schematically depicted in Fig. 4. In the contributions from the first two diagrams, which proceed through the intermediate resonances $\rho \to a_1\pi$ and $\rho \to f_0\rho$, respectively (where ρ stands for $\rho(770)$ and its radial excitations), only the parameters of the current were adopted to the improved data and a new ρ

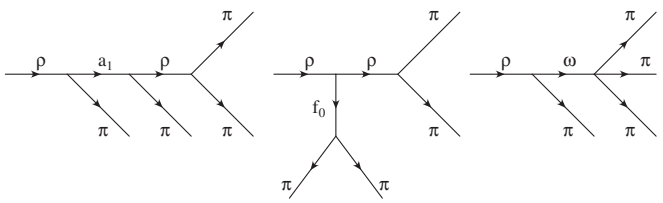

FIG. 4. Diagrams contributing to the hadronic current in [5].

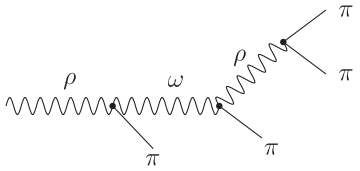

FIG. 5. The new contributions from the omega part of the current.

resonance $[\rho(2040)]$ was added (necessary to fit the *BABAR* [16] data). The contribution from ω, where previously the substructure of the omega decay was not taken into account, is now modeled using information from [28]. Schematically, the new ω amplitude is depicted in Fig. 5.

BABAR has, furthermore, observed [17] a strong $\rho^+\rho^-$ contribution. Thus a new part containing the $\rho \to \rho\rho$ contribution has been added, treating the ρ particles like $SU(2)$ gauge bosons. The contributions to the amplitude are depicted in Fig. 6. For more general frameworks, where such terms are present see [30] (and references therein). The SU(2) symmetric Lagrangian describing $\rho-$ pair production reads

$$\mathcal{L}_\rho = \tfrac{1}{4}\vec{F}_{\mu\nu}\cdot\vec{F}^{\mu\nu} + \tfrac{1}{2}(\vec{D^\mu}\phi)\cdot(\vec{D_\mu}\phi) + \tfrac{1}{2}m_\pi^2\vec{\phi}\cdot\vec{\phi} + \tfrac{1}{2}m_\rho^2\vec{\rho}_\mu\cdot\vec{\rho}^\mu, \tag{15}$$

where

$$\vec{\phi} = \begin{pmatrix} \frac{1}{\sqrt{2}}(\pi^+ + \pi^-) \\ \frac{i}{\sqrt{2}}(\pi^+ - \pi^-) \\ \pi^0 \end{pmatrix}, \qquad \vec{\rho}_\mu = \begin{pmatrix} \frac{1}{\sqrt{2}}(\rho^+ + \rho^-) \\ \frac{i}{\sqrt{2}}(\rho^+ - \rho^-) \\ \rho^0 \end{pmatrix}_\mu,$$

$$\vec{F}_{\mu\nu} = \partial_\mu\vec{\rho}_\nu - \partial_\nu\vec{\rho}_\mu - g\vec{\rho}_\mu\times\vec{\rho}_\nu, \tag{16}$$

and

$$\vec{D_\mu}\phi = \partial_\mu\vec{\phi} + g(\vec{\rho}_\mu\times\vec{\phi}). \tag{17}$$

The only free parameter, the coupling constant g ($g = g_{\rho\pi\pi}$), can be extracted from $\rho \to \pi\pi$ decay. However, as it stands, the model leads to a wrong high-energy behavior of the cross section, falling less rapidly than the data. This problem can be cured by adding ρ' contributions and allowing for trilinear couplings between ρ and ρ'. It was also necessary to relax the fixed coupling g to fit the data. The detailed description can be found in the Appendix. The

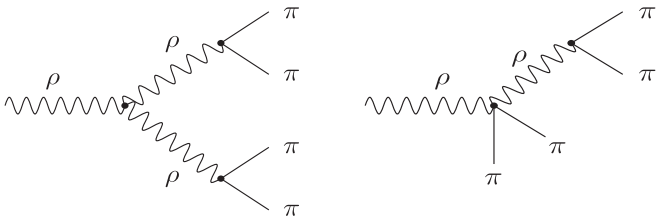

FIG. 6. The new contributions from ρ mesons.

model can be further refined, when more experimental information is available.

The behavior of the four-pion amplitude in the low Q^2 region has also been studied [6] in the framework of chiral resonance theory, including terms up to $O(p^4)$ [31]. The implementation of resonances and their parameters differs from the choice in this paper. The results of the two models are compared to the data in Figs. 10 and 11.

V. FIT OF THE CURRENT PARAMETERS TO THE EXPERIMENTAL DATA

To separate the well-measured ω contribution, from the rest, we fitted the parameters of the model to the ω part of the cross section of the reaction $e^+e^- \to 2\pi^0\pi^+\pi^-$ extracted from preliminary *BABAR* data [17]. Furthermore, we fitted the model parameters to the cross sections of the reactions $e^+e^- \to 2\pi^0\pi^+\pi^-$ and $e^+e^- \to 2\pi^+2\pi^-$ measured by *BABAR* [16,17].

The results are shown in Figs. 7–9 and in Table II. The fit is quite good, with $\chi^2/n_{\mathrm{d.o.f}} = 275/287$. However, one has to remember that only the cross sections were fitted and all subdistributions are to large extent determined by the model assumptions. The constants $\beta_i^{a_1}$, $\beta_i^{f_0}$, and β_i^{ω} (with $i = 1, 2, 3$) characterize the relative importance of the radial ρ excitations (compared to the one of the ground state, $\beta_0 \equiv 1$) in the amplitudes depicted in Figs. 4 and 5 [see also Eq. (A11)]. Large values of $\beta_i^{f_0}$ are the consequence of the small $f_0(1370) - \rho_0 - \rho_0$ coupling compared to higher ρ radial excitations, which are indeed dominated by ρ_1.

It is interesting to see how the model compares to predictions based on the chiral Lagrangian [6] in the low

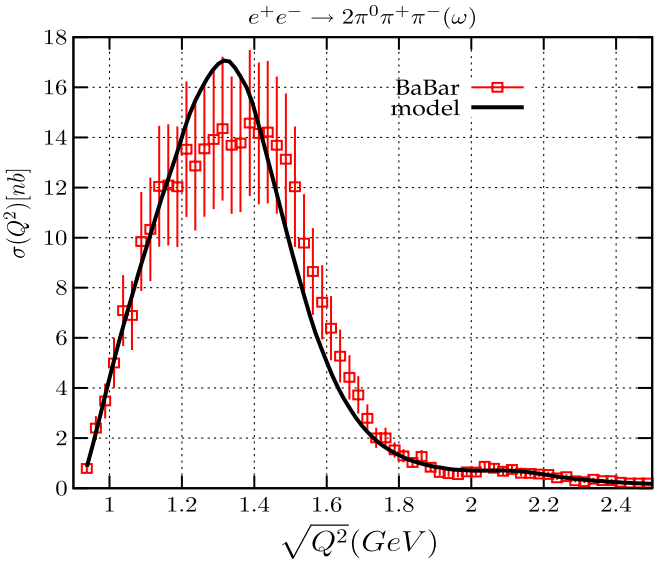

FIG. 7 (color online). Fit to the $\omega-$ part of the cross section for $e^+e^- \to 2\pi^0\pi^+\pi^-$ [17] (20% systematical error for the preliminary *BABAR* data was assumed).

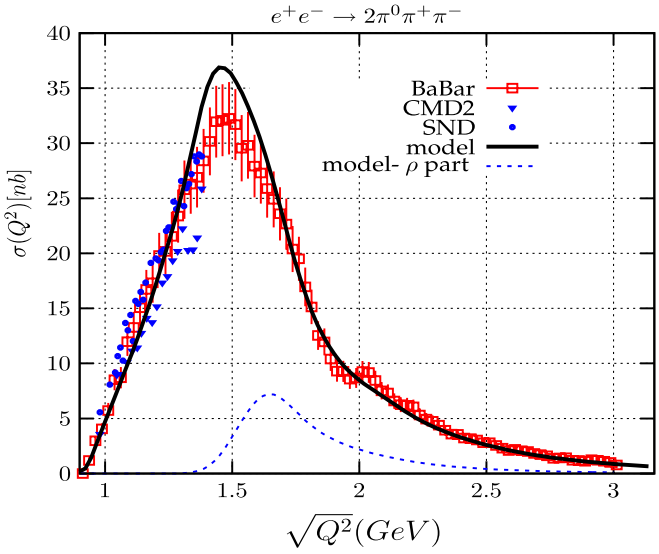

FIG. 8 (color online). Fit to the data for $\sigma(e^+e^- \to 2\pi^0\pi^+\pi^-)$, taken from [17] (10% systematical error was added to the statistical error). For comparison also CMD2 [10] and SND [13] data, which are consistent with *BABAR* data, are shown (without their 10%–20% error bars). Contributions from ρ part of the current [Eq. (A8)] to the cross section (see text for definition) are also shown.

Q^2 region, where this ansatz is expected to be applicable. In Fig. 10 (Fig. 11) this comparison is shown for the charged (neutral) mode, together with data from *BABAR* [16,17], CMD2 [10,12,14], and SND [13]. Since our model parameters were fitted to that cross section the thick dotted curve is not a prediction, apart of the $\sqrt{Q^2}$ region below

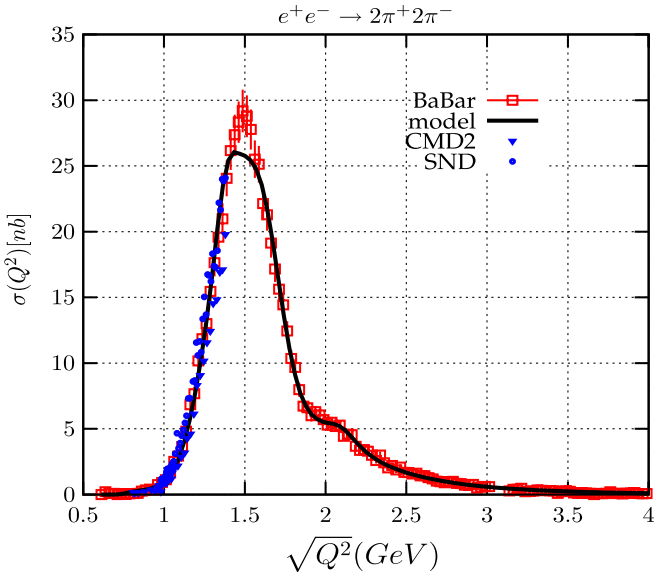

FIG. 9 (color online). Fit to the data for $\sigma(e^+e^- \to 2\pi^+2\pi^-)$, taken from [16]. For comparison also CMD2 [10,12,14] and SND [13] data, which are consistent with *BABAR* data, are shown (without their 7%–20% error bars).

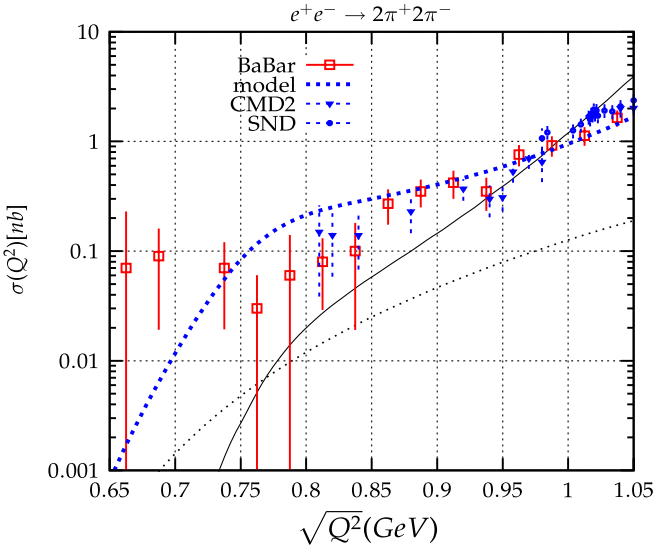

FIG. 10 (color online). Comparison of our model with the chiral Lagrangian [6] predictions (solid and dotted lines) in low-energy region and experimental data [12–14,16].

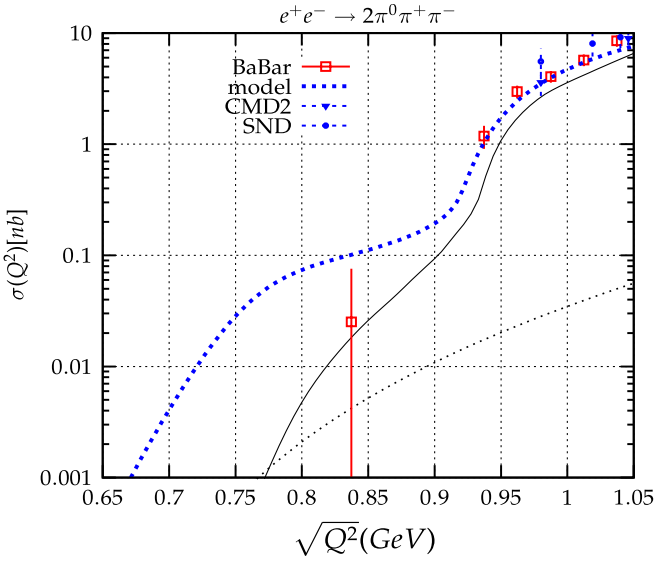

FIG. 11 (color online). Comparison of our model with the chiral Lagrangian [6] predictions (solid and dotted lines) in low-energy region and experimental data [10,13,17].

0.8 GeV, from where the contribution to χ^2 of the fit is negligible due to the low accuracy of the data.

The subdistributions can be qualitatively compared (Fig. 12) with plots presented by *BABAR* [16]. These were not used in the fit and thus can be considered as predictions. Integrals for both experimental and theoretical plots are equal by construction. Further refinements of the model will be possible when the data on subdistributions will become available.

The contributions from two ρ mesons in the final state are shown as dashed line in Fig. 8. They were extracted selecting events with $\pi^+\pi^0$ and $\pi^-\pi^0$ invariant masses within the range from $m_\rho - \Gamma_\rho$ to $m_\rho + \Gamma_\rho$. These are affected by background from the other amplitudes and thus do not correspond exactly to the contributions from ρ part of the current [Fig. 6 and Eq. (A8)], hence the separation is not as clean as for the ω case. The model prediction is smaller than the *BABAR* result [17].

Selected two- and three-pion invariant mass subdistributions for the reaction $e^+e^- \to 2\pi^0\pi^+\pi^-\gamma(\gamma)$ are shown in Fig. 13. The contributions from various resonances included in the model are clearly visible. Comparisons of the predictions will be possible, when the final *BABAR* results are published.

VI. MODEL PREDICTIONS FOR τ DECAYS

One can confront the model with the data [32] for the partial τ decay rates to four-pion final states. The results are collected in Table I. The theoretical error is obtained from the errors of the model parameters extracted in the fit. Within the quoted errors, the predictions are in good agreement with the data even if one observes sizable difference between the data for $Br(\tau^- \to \nu_\tau 2\pi^-\pi^+\pi^0)$ and the prediction via the isospin relations. At present the results are still consistent within the conservatively estimated error, which is dominated by the one of the preliminary *BABAR* result for $\sigma(e^+e^- \to 2\pi^0\pi^+\pi^-)$. With an expected error of about 5%, the final *BABAR* result will further push the accuracy of the isospin symmetry tests.

The model of 4π hadronic current proposed in this paper was fitted to *BABAR* data and relies on isospin symmetry. Thus its predictions for the τ spectral functions follows the predictions from *BABAR* data based on the isospin symmetry assumption (presented in Section III), apart from few percent phase space effects coming from the $\pi^\pm - \pi^0$ mass difference. The model predictions are also shown in Fig. 1–3. The central curve represents the model predictions, the upper and lower curves are the error estimates based on errors coming from the fitted parameters of the model.

Two, three and four-pion invariant mass distributions obtained within our model are compared with CLEO data (available only as plots) in Fig. 14. Although predictions and the data differ as far as the detailed description is concerned, good qualitative agreement is observed.

VII. IMPLEMENTATION INTO PHOKHARA AND TESTS OF THE MONTE CARLO GENERATOR

The model for the hadronic current was implemented into the PHOKHARA event generator (version 7.0). It will be available at http://ific.uv.es/ rodrigo/phokhara/ together with the implementation of the J/ψ and $\psi(2S)$ contributions to 2-body hadronic final states (in preparation). Only the current J_μ was coded in the form described in the

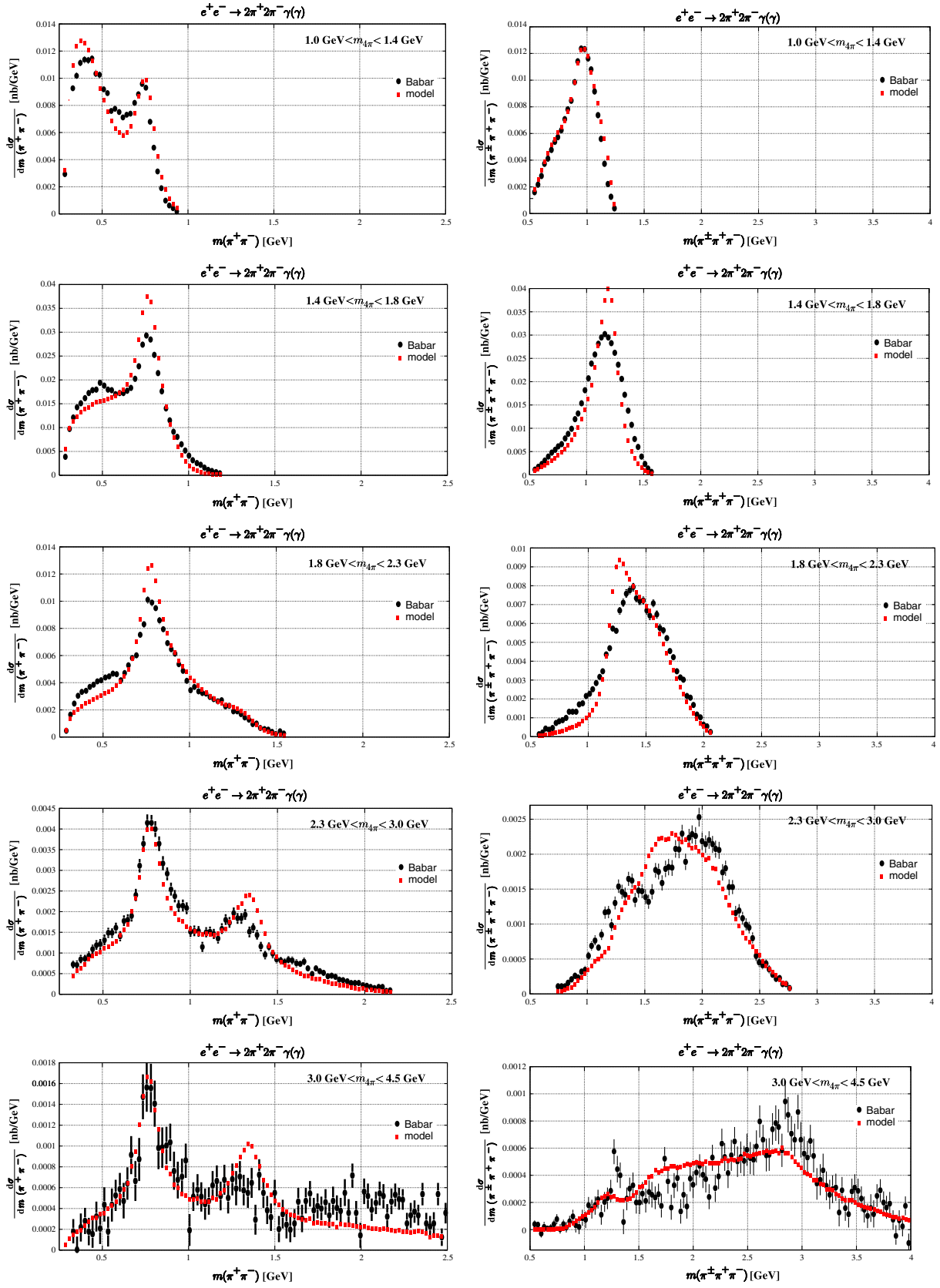

FIG. 12 (color online). Two- and three-pion invariant mass distributions for five different ranges of $2\pi^+2\pi^-$ invariant mass. The *BABAR* data points (filled circles), given as events/bin, are superimposed on plots obtained by PHOKHARA (filled squares) (see text for details).

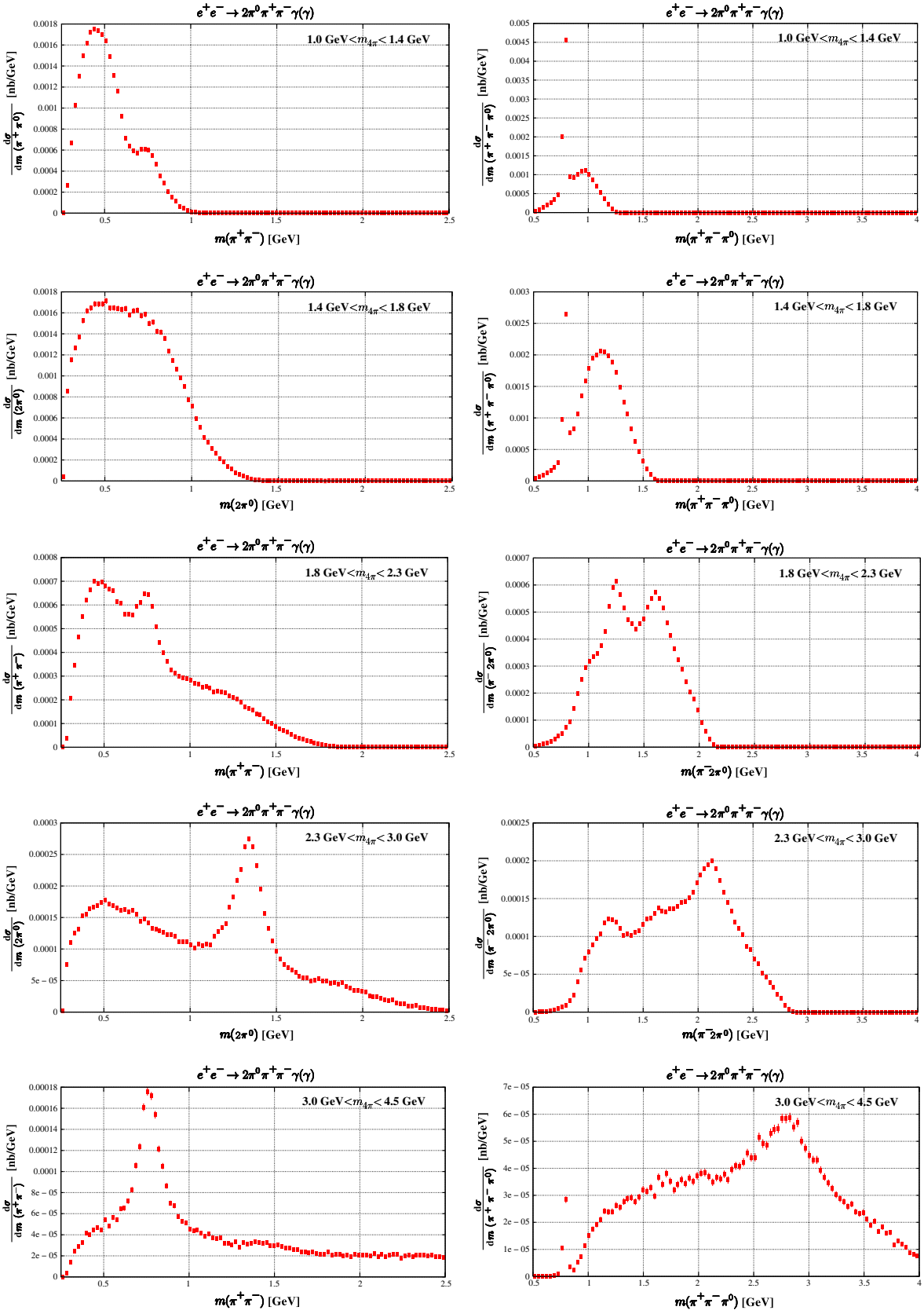

FIG. 13 (color online). Predicted by the model two- and three-pion invariant mass distributions for five different ranges of $2\pi^0\pi^+\pi^-$ invariant mass (selected set).

TABLE I. Branching ratios of τ decay modes. Results of our model are compared to experimental data [32] and predictions based on *BABAR* data [16,17] and isospin symmetry.

	$Br(\tau- \to \nu_\tau 2\pi^-\pi^+\pi^0)$	$Br(\tau- \to \nu_\tau \pi^-\omega(\pi^-\pi^+\pi^0))$	$Br(\tau- \to \nu_\tau \pi^- 3\pi^0)$
PDG [32]	$(4.46 \pm 0.06)\%$	$(1.77 \pm 0.1)\%$	$(1.04 \pm 0.08)\%$
Model	$(4.12 \pm 0.21)\%$	$(1.60 \pm 0.13)\%$	$(1.06 \pm 0.09)\%$
BABAR (CVC)	$(3.98 \pm 0.30)\%$	$(1.57 \pm 0.31)\%$	$(1.02 \pm 0.05)\%$

TABLE II. Values of the couplings masses and widths obtained in the fit. Masses and widths in GeV; couplings β_i^j, ($j = a_1,\ f_0,\ \omega$, and $i = 1, 2, 3$) as well as c_ρ are dimensionless; couplings c_{a_1} and c_{f_0} in GeV^{-2}; coupling c_ω in GeV^{-1}.

$\bar{m}_{\rho_1}$	1.437(2)	$\bar{m}_{\rho_2}$	1.738(12)	$\bar{m}_{\rho_3}$	2.12(2)
$\bar{\Gamma}_{\rho_1}$	0.520(2)	$\bar{\Gamma}_{\rho_2}$	0.450(9)	$\bar{\Gamma}_{\rho_3}$	0.30(2)
$\beta_1^{a_1}$	$-0.066(3)$	$\beta_2^{a_1}$	$-0.021(1)$	$\beta_3^{a_1}$	
$\beta_1^{f_0}$	$7(6)\cdot 10^4$	$\beta_2^{f_0}$	$-2.5(5.0)\cdot 10^3$	$\beta_3^{f_0}$	$1.9(1.6)\cdot 10^3$
β_1^{ω}	$-0.33(8)$	β_2^{ω}	0.012(3)	β_3^{ω}	$-0.0053(7)$
c_{a_1}	$-225(3)$	c_{f_0}	64(3)	c_ω	$-1.47(4)$
c_ρ	$-2.46(3)$	χ^2	275	$n_{\mathrm{d.o.f}}$	287

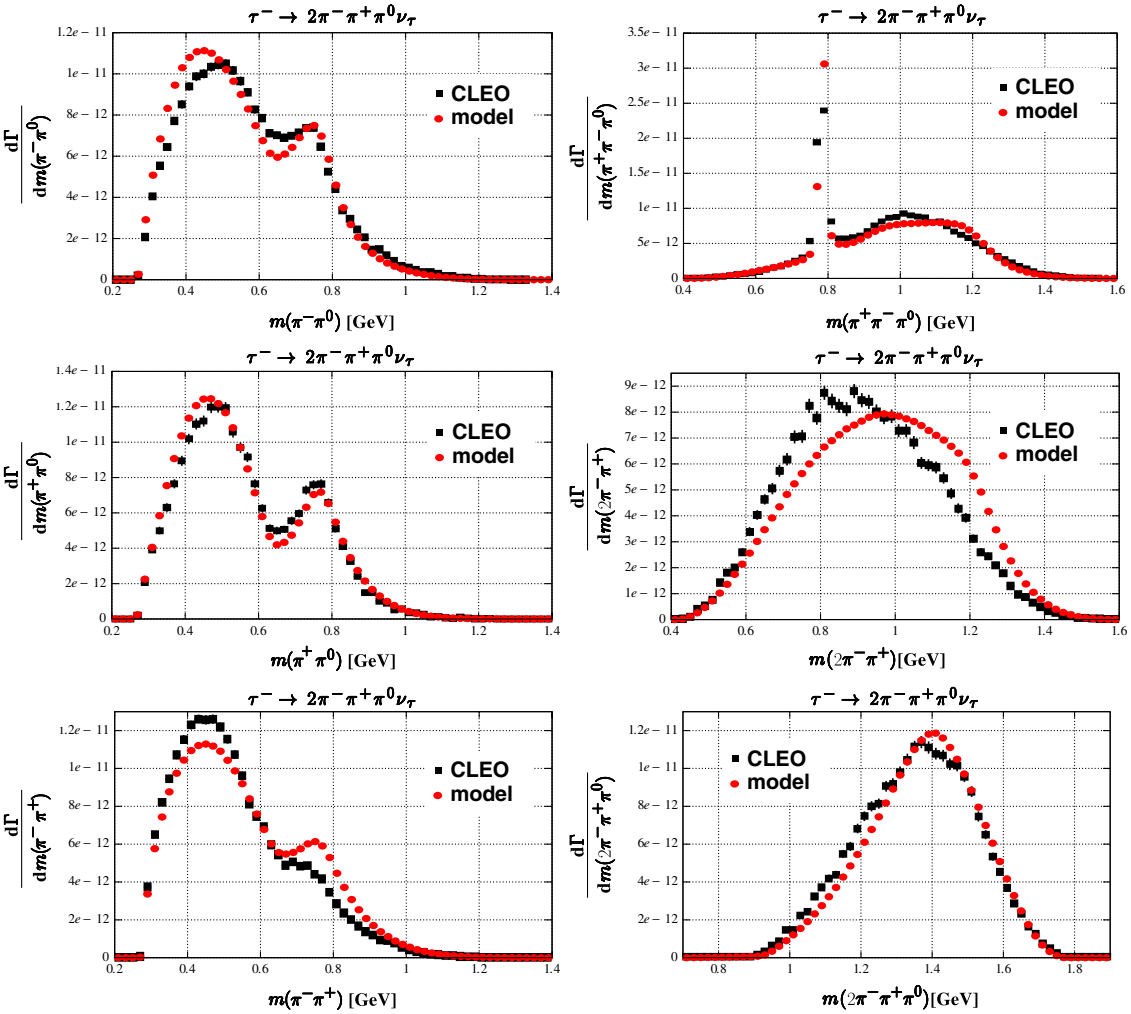

FIG. 14 (color online). Two- and three-pion invariant mass subdistributions for different pion charge combinations. The CLEO data points (filled circles), given as events/bin, are superimposed on plots obtained within studied model (filled squares). See text for details.

Appendix; the charged mode is obtained via the relation Eq. (3). Neither the ω- part of the current nor the double ρ resonance diagrams (left in Fig. 6) contribute to that part. Only *a priori* weights, used in the multichannel Monte Carlo generation, were changed as compared to previous versions [23]. Nevertheless, tests checking the implementation were performed to assure a proper technical precision of the code. The next-to-leading order (NLO) version of the code was checked for the configurations without any cuts against analytic NLO results of [33] (see also [23]), separately for one- and two-photon contributions. The separation $w = \frac{E_\gamma}{\sqrt{s}} = 10^{-4}$ between soft (integrated analytically) and hard (generated) parts was used in this test. The precision of the tests, limited by the Monte Carlo statistics, is significantly below one per mill. As the analytic formula contains as a factor the cross section of the process without photon emission ($\sigma(e^+e^- \to 4\pi)$), which is not known analytically, it was obtained by means of Monte Carlo integration by a dedicated program. In that program, in contrast to PHOKHARA, flat phase space generation was used to avoid any errors due to the change of variables. The independence of the results of the generation on the separation into soft and hard parts was also tested with similar precision.

VIII. CONCLUSIONS

Four-pion production in e^+e^- annihilation and in τ decays is characterized by a multitude of resonant subchannels. This makes it difficult to construct an amplitude which is based on first principles of QCD only. In this paper we have constructed a model amplitude which incorporates a limited set of channels, namely, $a_1\pi$, ρf_0, $\rho\rho$, and $\omega\pi$ and which is approximately consistent with chiral predictions for small Q^2. A number of parameters which characterize the relative importance of the various couplings and of the radial excitations of the ρ meson is fitted to the cross sections for $2\pi^+2\pi^-$ and $\pi^+\pi^-2\pi^0$ as measured by the *BABAR* collaboration. The model predictions for the two- and three-pion mass distributions which are not fitted separately, are consistent with the data both from e^+e^- annihilation and from τ decays. Furthermore, we find that the present data are, within their 5%–10% systematic error, consistent with the relations derived from isospin invariance, and which are intrinsic for our model. The amplitude is incorporated into the Monte Carlo generator PHOKHARA, simulating 4π production through the radiative return.

ACKNOWLEDGMENTS

We are grateful to Achim Denig for numerous discussions and reading of the manuscript. H. C. and A. W. are grateful for the support and the kind hospitality of the Institut für Theoretische Teilchenphysik of the Karlsruhe University. This work is supported in part by BMBF Grant No. 05HT4VKA/3, EU 6th Framework Program under Contract No. MRTN-CT-2006-035482 (FLAVIAnet), TARI Project No. RII3-CT-2004-506078, Polish State Committee for Scientific Research (KBN) under Contract No. 1 P03B 003 28.

APPENDIX: THE CURRENT

In this Appendix we give a complete definition of the hadronic current used in this paper. We take as a basic building block the electromagnetic current $J^{em}_\mu = \frac{1}{\sqrt{2}} J^3_\mu$ (using $J^{I=0}_\mu = 0$), which is of direct importance for implementation in PHOKHARA and define $\Gamma^\mu \equiv \frac{1}{\sqrt{2}} \times \langle \pi^+\pi^-\pi^0_1\pi^0_2|J^3_\mu|0\rangle$. Other channels can be obtained through Eq. (3).

Γ^μ can be decomposed into the following four parts:

$$\Gamma^\mu = \Gamma^\mu_{a_1} + \Gamma^\mu_{f_0} + \Gamma^\mu_\omega + \Gamma^\mu_\rho. \tag{A1}$$

We denote the four-pion momenta by $q_1(\pi^0)$, $q_2(\pi^0)$, $q_3(\pi^-)$ and $q_4(\pi^+)$ and use the proper pion masses $m_{\pi^\pm}$ and m_{π^0} wherever appropriate. Thus the current possesses isospin symmetry, broken only by kinematic effects. The general structure is largely based on [5]. Contribution from the part containing an a_1 exchange reads

$$\begin{aligned}\Gamma^\mu_{a_1}(q_1, q_2, q_3, q_4) = {} & \tilde\Gamma^\mu_{a_1}(q_3, q_2, q_1, q_4) \\ & + \tilde\Gamma^\mu_{a_1}(q_3, q_1, q_2, q_4) \\ & - \tilde\Gamma^\mu_{a_1}(q_4, q_2, q_1, q_3) \\ & - \tilde\Gamma^\mu_{a_1}(q_4, q_1, q_2, q_3).\end{aligned} \tag{A2}$$

The function $\tilde\Gamma^\mu_{a_1}$ is of the form

$$\begin{aligned}\tilde\Gamma^\mu_{a_1}(q_1, q_2, q_3, q_4) = {} & c_{a_1} F_\rho(Q^2, \vec\beta^{a_1}) BW_{a_1}((Q - q_1)^2) \\ & \times B_\rho((q_3 + q_4)^2)\Big[(q_3 - q_4)^\mu \\ & + q_1^\mu \frac{q_2(q_3 - q_4)}{(Q - q_1)^2} - Q^\mu\Big(\frac{Q(q_3 - q_4)}{Q^2} \\ & + \frac{(Qq_1)(q_2(q_3 - q_4))}{Q^2(Q - q_1)^2}\Big)\Big],\end{aligned} \tag{A3}$$

and corresponds to the configuration $\rho(Q) \to \pi(q_1)a_1(\to \rho\pi(q_2))$ with $\rho \to \pi(q_3)\pi(q_4)$. The other three terms are enforced by Bose symmetry ($q_1 \to q_2$) and charge conjugation.

The contribution from $\rho \to f_0(\pi(q_1)\pi(q_2))\rho(\to \pi(q_3)\pi(q_4))$ reads

$$\Gamma^{\mu}_{f_0}(q_1,q_2,q_3,q_4) = c_{f_0}F_\rho(Q^2,\vec{\beta}^{f_0})T_\rho((q_3+q_4)^2) \times BW_{f_0}((q_1+q_2)^2)\Big[(q_3-q_4)^\mu - Q^\mu\frac{Q(q_3-q_4)}{Q^2}\Big]. \quad \text{(A4)}$$

The contribution coming from the anomalous part of the current (containing ω exchange) reads

$$\Gamma^{\mu}_{\omega}(q_1,q_2,q_3,q_4) = \tilde{\Gamma}^{\mu}_{\omega}(q_1,q_2,q_3,q_4) + \tilde{\Gamma}^{\mu}_{\omega}(q_2,q_1,q_3,q_4), \quad \text{(A5)}$$

with

$$\tilde{\Gamma}^{\mu}_{\omega}(q_1,q_2,q_3,q_4) = 2c_\omega g_{\omega\pi\rho}g_{\rho\pi\pi}F_\rho(Q^2,\vec{\beta}^{\omega}) \times BW_\omega((Q-q_1)^2)H_\rho((q_2+q_3)^2, (q_2+q_4)^2,(q_3+q_4)^2)[q_2^\mu((q_1q_4) \times (q_3Q)-(q_1q_3)(q_4Q)) + q_3^\mu((q_1q_2) \times (q_4Q)-(q_1q_4)(q_2Q)) + q_4^\mu((q_1q_3) \times (q_2Q)-(q_1q_2)(q_3Q))], \quad \text{(A6)}$$

where

$$g_{\omega\pi\rho} = 42.3\ \text{GeV}^{-5}, \qquad g_{\rho\pi\pi} = 5.997. \quad \text{(A7)}$$

The first term in Eq. (A5) corresponds to the configuration $\rho \to \pi(q_1)\omega(\to \pi(q_2)\pi(q_3)\pi(q_4))$; the second follows from the Bose symmetry.

The structure of the omega decay was taken from [28]. Other possible contributions to the 3π part of the current coming from $\phi(1020)$ or higher radial ω excitations are not seen in the data and thus were not included into the model.

Γ^{μ}_{ρ} part of the current is of the following form:

$$\Gamma^{\mu}_{\rho}(q_1,q_2,q_3,q_4) = c_\rho g^3_{\rho\pi\pi}g_{\rho\gamma}BW^{\rho_0,\rho_1}(Q^2)\Big(g^\mu_\nu - \frac{Q^\mu Q_\nu}{Q^2}\Big) \times\{[(G^\nu_\rho(q_1,q_2,q_3,q_4) + G^\nu_\rho(q_4,q_1,q_2,q_3)) - (3\leftrightarrow 4)] + [1\leftrightarrow 2]\}, \quad \text{(A8)}$$

where

$$G^{\mu}_{\rho}(q_1,q_2,q_3,q_4) = q_1^\mu BW^{\rho_0,\rho_1}((q_1+q_3)^2) \times [BW^{\rho_0,\rho_1}((q_2+q_4)^2) \times (Q+2q_3)(q_2-q_4)+2], \quad \text{(A9)}$$

and

$$BW^{\rho_0,\rho_1}(p^2) = BW_3(p^2,m_\rho,\Gamma_\rho)/m^2_{\rho_0} - BW_3(p^2,m_{\rho_1},\Gamma_{\rho_1})/m^2_{\rho_1}. \quad \text{(A10)}$$

For the $\rho-\gamma^*$ coupling we use $g_{\rho\gamma} = 0.1212\ \text{GeV}^2$. The double resonant terms disappear in the (-000) and $(++--)$ channels, the single resonant contribution, however, remains.

For completeness we list all propagators required for the current. A new ρ_3 contribution was included in $F_\rho(Q^2)$ only. The different ρ propagators T_ρ, F_ρ, and B_ρ are used in the current due to the fact that the ρ may couple in a different way to different resonances and the propagators themselves contain indirectly some information about the couplings.

$$F_\rho(Q^2,\vec{\beta}) = \frac{1}{1+\beta_1+\beta_2+\beta_3}[BW_3(Q^2,m_\rho,\Gamma_\rho) + \beta_1 BW_3(Q^2,\bar{m}_{\rho_1},\bar{\Gamma}_{\rho_1}) + \beta_2 BW_3(Q^2,\bar{m}_{\rho_2},\bar{\Gamma}_{\rho_2}) + \beta_3 BW_3(Q^2,\bar{m}_{\rho_3},\bar{\Gamma}_{\rho_3})], \quad \text{(A11)}$$

where $\vec{\beta} = (\beta_1,\beta_2,\beta_3)$ and

$$BW_3(Q^2,m_\rho,\Gamma_\rho) = \frac{m^2_\rho}{m^2_\rho - Q^2 - i\Gamma_\rho m_\rho\sqrt{\frac{m^2_\rho}{Q^2}}\left[\frac{Q^2-4m^2_\pi}{m^2_\rho-4m^2_\pi}\right]^3}. \quad \text{(A12)}$$

Only the masses $\bar{m}_{\rho_i}$ and the widths $\bar{\Gamma}_{\rho_i}$ of ρ_1, ρ_2, and ρ_3 that appear in $F_\rho(Q^2,\vec{\beta})$ were fitted to the data. The results are listed in Table II.

For the masses and the widths of particles in all other parts of the current we use their PDG values:

$$\begin{aligned} m_\rho &= 0.7755\ \text{GeV}, & \Gamma_\rho &= 0.1494\ \text{GeV},\\ m_{\rho_1} &= 1.459\ \text{GeV}, & \Gamma_{\rho_1} &= 0.4\ \text{GeV},\\ m_{\rho_2} &= 1.72\ \text{GeV}, & \Gamma_{\rho_2} &= 0.25\ \text{GeV}, \end{aligned} \quad \text{(A13)}$$

$$B_\rho(Q^2) = [BW_3(Q^2,m_\rho,\Gamma_\rho) + \beta BW_3(Q^2,m_{\rho_1},\Gamma_{\rho_1})]/(1+\beta), \quad \text{(A14)}$$

with

$$\beta = -0.145. \quad \text{(A15)}$$

The a_1 propagator reads

$$BW_{a_1}(Q^2) = \frac{m^2_{a_1}}{m^2_{a_1} - Q^2 - i\Gamma_{a_1}m_{a_1}\frac{g(Q^2)}{g(m^2_{a_1})}}, \quad \text{(A16)}$$

with [5,34]

$$g(Q^2) = 1.623Q^2 + 10.38 - \frac{9.32}{Q^2} + \frac{0.65}{(Q^2)^2} \quad \text{for } Q^2 > (m_{a_1} + m_\pi)^2,$$
$$g(Q^2) = 4.1(Q^2 - 9m_\pi^2)^3[1\text{–}3.3(Q^2 - 9m_\pi^2) + 5.8(Q^2 - 9m_\pi^2)^2] \quad \text{for } Q^2 < (m_{a_1} + m_\pi)^2 \tag{A17}$$

(Q^2 in GeV^2) and

$$m_{a_1} = 1.23 \text{ GeV}, \qquad \Gamma_{a_1} = 0.2 \text{ GeV}. \tag{A18}$$

$$T_\rho(Q^2) = [BW_3(Q^2, m_\rho, \Gamma_\rho) + \bar\beta_1 BW_3(Q^2, m_{\rho_1}, \Gamma_{\rho_1}) + \bar\beta_2 BW_3(Q^2, m_{\rho_2}, \Gamma_{\rho_2})]/(1 + \bar\beta_1 + \bar\beta_2), \tag{A19}$$

where

$$\bar\beta_1 = 0.08, \qquad \bar\beta_2 = -0.0075. \tag{A20}$$

The f_0 meson propagator chosen to be

$$BW_{f_0}(Q^2) = \frac{m_{f_0}^2}{m_{f_0}^2 - Q^2 - i\Gamma_{f_0} m_{f_0} \sqrt{\frac{m_{f_0}^2}{Q^2}\frac{Q^2 - 4m_\pi^2}{m_{f_0}^2 - 4m_\pi^2}}}, \tag{A21}$$

where

$$m_{f_0} = 1.35 \text{ GeV}, \qquad \Gamma_{f_0} = 0.2 \text{ GeV}. \tag{A22}$$

$$H_\rho(Q_1^2, Q_2^2, Q_3^2) = BW_3(Q_1^2, m_\rho, \Gamma_\rho) + BW_3(Q_2^2, m_\rho, \Gamma_\rho) + BW_3(Q_3^2, m_\rho, \Gamma_\rho). \tag{A23}$$

$$BW_\omega(Q^2) = \frac{m_\omega^2}{m_\omega^2 - Q^2 - i m_\omega \Gamma_\omega} \tag{A24}$$

is the ω meson propagator with

$$m_\omega = 0.78265 \text{ GeV}, \qquad \Gamma_\omega = 0.00849 \text{ GeV}. \tag{A25}$$

To obtain the correct chiral limit [6] of the current equation (A1) the following relations should hold

$$c_{a_1} = -\frac{4}{3}\frac{1}{f_\pi^2}$$
$$c_{f_0} + \frac{3}{2}c_{a_1} = 4c_\rho g_{\rho\pi\pi}^3 g_{\rho\gamma}\left(\frac{1}{m_{\rho_0}^2} - \frac{1}{m_{\rho_1}^2}\right)^2, \tag{A26}$$

where $f_\pi = 0.0924$ GeV. Comparing the fitted value

$$c_{a_1}^{\text{fit}} = -225(3) \text{ GeV}^{-2}, \tag{A27}$$

with its proper chiral limit

$$c_{a_1} \simeq -156 \text{ GeV}^{-2}, \tag{A28}$$

and also the second relation from Eq. (A26) as obtained in the fit

$$c_{f_0}^{\text{fit}} + \frac{3}{2}c_{a_1}^{\text{fit}} = -273(5) \text{ GeV}^{-2},$$
$$4c_\rho^{\text{fit}} g_{\rho\pi\pi}^3 g_{\rho\gamma}\left(\frac{1}{m_{\rho_0}^2} - \frac{1}{m_{\rho_1}^2}\right)^2 = -307(4) \text{ GeV}^{-2}, \tag{A29}$$

it is clear that they hold only approximately. This reflects the fact that the fit was performed in a Q^2-region, where the chiral Lagrangian leads, at best, to an approximate treatment, and that furthermore higher order terms are present.

[1] R. Fischer, J. Wess, and F. Wagner, Z. Phys. C **3**, 313 (1980).
[2] R. Decker, Z. Phys. C **36**, 487 (1987).
[3] R. Decker, M. Finkemeier, P. Heiliger, and H. H. Jonsson, Z. Phys. C **70**, 247 (1996).
[4] J. H. Kühn, Nucl. Phys. B, Proc. Suppl. **76**, 21 (1999).
[5] H. Czyż and J. H. Kühn, Eur. Phys. J. C **18**, 497 (2001).
[6] G. Ecker and R. Unterdorfer, Eur. Phys. J. C **24**, 535 (2002).
[7] M. Davier, S. Eidelman, A. Hocker, and Z. Zhang, Eur. Phys. J. C **27**, 497 (2003).
[8] A. E. Bondar, S. I. Eidelman, A. I. Milstein, T. Pierzchala, N. I. Root, Z. Was, and M. Worek, Comput. Phys. Commun. **146**, 139 (2002).
[9] M. Davier, A. Hocker, and Z. Zhang, Rev. Mod. Phys. **78**, 1043 (2006).
[10] R. R. Akhmetshin *et al.* (CMD2 Collaboration), Phys. Lett. B **466**, 392 (1999).
[11] K. W. Edwards *et al.* (CLEO Collaboration), Phys. Rev. D **61**, 072003 (2000).
[12] R. R. Akhmetshin *et al.* (CMD-2 Collaboration), Phys. Lett. B **475**, 190 (2000).
[13] M. N. Achasov *et al.*, Zh. Eksp. Teor. Fiz. **123**, 899 (2003) [J. Exp. Theor. Phys. **96**, 789 (2003)].
[14] R. R. Akhmetshin *et al.* (CMD-2 Collaboration), Phys. Lett. B **595**, 101 (2004).
[15] S. Schael *et al.* (ALEPH Collaboration), Phys. Rep. **421**, 191 (2005).
[16] B. Aubert *et al.* (*BABAR* Collaboration), Phys. Rev. D **71**, 052001 (2005).
[17] A. Petzold, presentation at EPS Conference, Manchester 2007; V. P. Druzhinin, arXiv:0710.3455.
[18] F. Jegerlehner, *The Anomalous Magnetic Moment of the Muon*, Springer Tracts in Modern Physics Vol. 226 (Springer-Verlag, Berlin, Heidelberg, 2008).
[19] K. Melnikov and A. Vainshtein, *Theory of the Muon Anomalous Magnetic Moment*, Springer Tracts in

Modern Physics Vol. 216 (Springer-Verlag, Berlin, Heidelberg, 2006).
[20] Min-Shih Chen and P. M. Zerwas, Phys. Rev. D **11**, 58 (1975).
[21] S. Binner, J. H. Kühn, and K. Melnikov, Phys. Lett. B **459**, 279 (1999).
[22] G. Rodrigo, H. Czyż, J. H. Kühn, and M. Szopa, Eur. Phys. J. C **24**, 71 (2002).
[23] H. Czyż, A. Grzelinska, J. H. Kühn, and G. Rodrigo, Eur. Phys. J. C **27**, 563 (2003).
[24] H. Czyż, A. Grzelińska, J. H. Kühn, and G. Rodrigo, Eur. Phys. J. C **33**, 333 (2004).
[25] H. Czyż, J. H. Kühn, E. Nowak, and G. Rodrigo, Eur. Phys. J. C **35**, 527 (2004).
[26] H. Czyż, A. Grzelińska, J. H. Kühn, and G. Rodrigo, Eur. Phys. J. C **39**, 411 (2005).
[27] H. Czyż, A. Grzelińska, and J. H. Kühn, Phys. Lett. B **611**, 116 (2005).
[28] H. Czyż, A. Grzelinska, J. H. Kühn, and G. Rodrigo, Eur. Phys. J. C **47**, 617 (2006).
[29] H. Czyż, A. Grzelinska, and J. H. Kühn, Phys. Rev. D **75**, 074026 (2007).
[30] M. Harada and K. Yamawaki, Phys. Rep. **381**, 1 (2003).
[31] G. Ecker, J. Gasser, A. Pich, and E. de Rafael, Nucl. Phys. **B321**, 311 (1989).
[32] W. M. Yao *et al.* (Particle Data Group), J. Phys. G **33**, 1 (2006).
[33] F. A. Berends, W. L. van Neerven, and G. J. H. Burgers, Nucl. Phys. **B297**, 429 (1988); **B304**, 921(E) (1988).
[34] J. H. Kühn and A. Santamaria, Z. Phys. C **48**, 445 (1990).